J. Phys.: Condens. Matter 4 (1992) 4323–4330. Printed in the UK

Low-temperature far-infrared study of localized states in In-doped $Pb_{0.75}Sn_{0.25}Te$ single crystals

N Romčević†, Z V Popović† and D R Khokhlov‡

† Institute of Physics, PO Box 57, 11001 Belgrade, Yugoslavia

‡ Low-Temperature Physics Department, Moscow State University, 117234 Moscow, Russia

Received 5 December 1991

Abstract. We present low-temperature far-infrared reflection spectra of In-doped $Pb_{0.75}Sn_{0.25}Te$ single crystals at various doping concentrations. These spectra at temperatures below 20 K are fitted using a modified plasmon–phonon interaction model with an additional oscillator, which describes the electron transition from two- to one-electron states at the In impurity level. The In-doped $Pb_{0.75}Sn_{0.25}Te$ impurity-state energy structure is explained.

1. Introduction

$Pb_{1-x}Sn_xTe$ is a well known narrow-band-gap semiconductor [1] with a usually very high ($n, p > 10^{17}$ cm^{-3}) intrinsic free-carrier concentration. In $A^{IV}B^{VI}$ alloys, indium concentrations higher than those of other donors and acceptors result in an impurity level the location of which is determined by alloy composition and temperature [2, 3]. The Fermi level of $A^{IV}B^{VI}$ alloys is pinned to the In impurity level and shifts with it on temperature and pressure changes [2]. Even though the pinning of the Fermi level to the In impurity level has been studied extensively [4, 5], no satisfactory explanation of this effect exists as yet. For $0.28 > x > 0.22$ the In impurity level lies within the forbidden band (dielectric states [2]), resulting in a sharp drop in the free-carrier concentration. These In-doped alloys are unique in that (at temperatures below about 20 K in the dielectric state) they are photosensitive and exhibit a decrease in electrical resistivity of several orders of magnitude when illuminated by low-intensity infrared radiation [6].

Because of their high free-carrier concentration, the optical properties of In-doped $Pb_{1-x}Sn_xTe$ in the far-infrared (FIR) spectral region have usually been investigated on thin-film samples [7] where a temperature-induced plasma frequency shift has been observed.

In our earlier paper [8] we analysed the FIR reflection spectra of a 0.5 at.% In-doped $Pb_{0.75}Sn_{0.25}Te$ single crystal and showed that, if a photo-excited free-carrier concentration spatial distribution is introduced into the plasmon–phonon interaction model, good agreement is obtained between the experimental and theoretical spectra. FIR spectra of the 1.2 at.% In-doped $Pb_{0.75}Sn_{0.25}Te$ single crystal are given in [9]. These spectra were analysed using a fitting procedure based on the plasmon–phonon interaction model. Below 20 K, a new structure is in evidence that has to be fitted

0953-8984/92/174323+08$04.50

by an additional oscillator in the plasmon–phonon interaction model. It may be explained in terms of $Pb_{0.75}Sn_{0.25}Te$ (In) localized impurity states.

In this paper, we present FIR reflection spectra of both 0.5 at.% and 1.2 at.% In-doped $Pb_{0.75}Sn_{0.25}Te$ single crystals from 50 to 250 cm^{-1} at temperatures of 5–20 K. The FIR spectra change with the In content and the infrared irradiating flux. These spectra are also analysed using a fitting procedure based on the modified plasmon–phonon interaction model (but incorporating an additional oscillator characterizing localized impurity states). Thus, the location of the impurity level at $T = 0$ K, the temperature T_k at which this level appears and its temperature dependence are obtained. The potential barrier width between localized states at $T = 0$ K and its value versus temperature as well as impurity-state-filling mechanisms are determined.

2. Experimental details

Indium-doped $Pb_{0.75}Sn_{0.25}Te$ single crystals grown by the modified Bridgman method were studied. Details of both the growth procedure and the measurement may be found in [8, 9]. A Bruker IFS 113v spectrometer with Oxford model CF 100 cryostat was used for the low-temperature FIR reflectivity measurements.

3. Results and discussion

Work to date on the persistent photoconductivity effect in In-doped $Pb_{0.75}Sn_{0.25}Te$ indicates that the effect occurs at temperatures below about 20 K, that it is most pronounced at indium concentrations of about 0.5 at.% and that the effect weakens with further increase in indium concentration [10]. Moreover, the quasi-stationary photo-excited carrier concentration is proportional to the incident irradiating flux Φ, if other parameters are constant. In an attempt to gain insight into how all the above are demonstrated in In-doped $Pb_{0.75}Sn_{0.25}Te$ reflection spectra, we present FIR reflectivity spectra at $T = 10$ K: figure 1(*a*) for 1.2 at.% In, figure 1(*b*) the same as for figure 1(*a*) but at $\Phi_2 = 0.75\Phi_1$ (a decrease in irradiation flux effected by a sample holder with a 25% smaller diaphragm surface) and figure 1(*c*) for 0.5 at.% In and $\Phi_3 = \Phi_1$. Although the spectra in figure 1 differ, a heretofore unobserved structure is clearly in evidence at about 130 cm^{-1} (indicated by arrows).

The reflectivity spectra shown in figure 1 were analysed using a fitting procedure based on the modified plasmon–phonon interaction model [9]:

$$\epsilon(\omega) = \epsilon_\infty \left[1 - \omega_p^2/\omega\left(\omega + i\tau^{-1}\right) + \left(\omega_{LO}^2 - \omega_{TO}^2\right)/\left(\omega_{TO}^2 - \omega^2 - i\gamma_{TO}\omega\right) + \omega_{loc}^2/\left(\omega_0^2 - \omega^2 - iG\omega\right)\right] \tag{1}$$

where ω_{TO}, ω_{LO} and ω_p are the transverse, longitudinal and plasma frequencies, respectively, γ_{TO} is the oscillator damping, τ is the free-carrier relaxation time and ϵ_∞ is the high-frequency dielectric constant. The second term in equation (1) is the free-carrier contribution and the third term is the lattice vibration contribution to the dielectric constant. The fourth term in equation (1) represents a new structure in the FIR reflection spectra due to an additional oscillator of characteristic frequency ω_0, where G is the damping and ω_{loc}^2 the 'strength' of this oscillator. The explanation of these parameters will be given below.

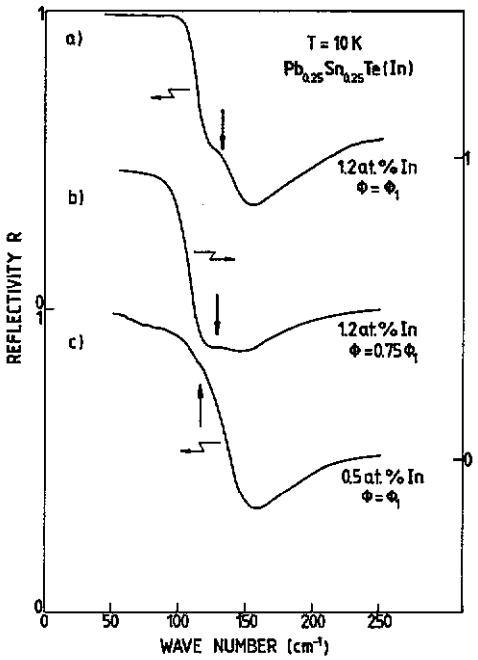

Figure 1. FIR reflection spectra of $Pb_{0.75}Sn_{0.25}Te$ (In) single crystals at $T = 10$ K: (*a*) $N_{In} = 1.2$ at.%, $\Phi_1 = \Phi$; (*b*) $N_{In} = 1.2$ at.%, $\Phi_2 = 0.75\Phi$; (*c*) $N_{In} = 0.5$ at.%, $\Phi_3 = \Phi$.

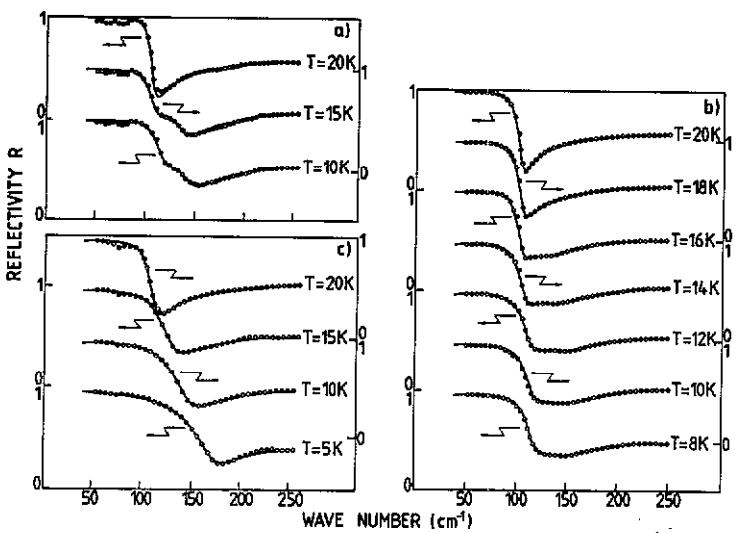

Figure 2. FIR reflection spectra of $Pb_{0.75}Sn_{0.25}Te$(In) single crystals at temperatures below $T = 20$ K, showing experimental spectra (○) and calculated spectra (——) obtained by a fitting procedure based on the model given by equation (1), with the parameter values given in table 1: (*a*) $N_{In} = 1.2$ at.%, $\Phi_1 = \Phi$; (*b*) $N_{In} = 1.2$ at.%, $\Phi_2 = 0.75\Phi$; (*c*) $N_{In} = 0.5$ at.%, $\Phi_3 = \Phi$.

As evidenced in figure 2, the computed spectra and experimental data are in reasonably good agreement. The best-fit parameters are listed in table 1. The parameters of the oscillators, $\omega_{TO} = 32$ cm^{-1}, $\omega_{LO} = 105$ cm^{-1} and $\gamma = 1$ cm^{-1},

are looked upon as constant because, as we previously discussed [9], their changes in such a narrow temperature interval are negligible. With regard to the fact that the changes $\epsilon_\infty = 44 \pm 2$ and $\tau^{-1} = 38 \pm 4$ cm^{-1} from specimen to specimen in this temperature interval are not great, we have not proceeded to discuss this separately. As can be seen from table 1, the parameter G depending on the In concentration drastically changes from 50 to 100. Moreover, when the flux changes, ω_p [8, 11] changes, and temperature changes affect ω_p, ω_0 and ω_{loc}.

Table 1 may be used to explain the difference between the spectra in figure 1. As the photo-excited electron concentration n in In-doped $Pb_{0.75}Sn_{0.25}Te$ is defined by the incident light flux, the n-value is higher in the case shown in figure 1(a) than in that in figure 1(b). This becomes evident if the ω_p-values listed in table 1 for the three cases are compared. Thus, because ω_p^2 is proportional to the total number of free carriers (both impurity and photo-excited), $\omega_{p3}(N_{In} = 0.5$ at.%, $\Phi) > \omega_{p1}(N_{In} = 1.2$ at.%, $\Phi) > \omega_{p2}(N_{In} = 1.2$ at.%, $0.75\Phi)$. This is substantiated in figure 3 which depicts the ω_p–temperature dependence for the three cases discussed.

Table 1. Optical parameters of phonons and plasmons obtained by oscillator fitting of the $Pb_{0.75}Sn_{0.25}Te$(In) reflection spectra.

T (K)	ω_p (cm^{-1})	ω_0 (cm^{-1})	ω_{loc}^2 (cm^{-2})	G (cm^{-1})	N_{In} (at.%)	Φ/Φ_1
10	84	135	1375			
15	71	125	1275	50	1.2	1
20	36	115	417			
8	73	139	1128			
10	68	136	1115			
12	63	133.1	1108			
14	48	127.1	1085	50	1.2	0.75
16	35	123.2	1001			
18	25	119.5	632			
20	19	115	254			
5	132	146	1154			
10	103	136	1132			
15	77	125	1041	100	0.5	1
20	37	115	347			

As ω_p and ω_0 in all three cases lie close to one another, small changes in ω_p have a great impact on the reflection spectra, i.e. the observability of the additional oscillator in figure 1. That is, for the case depicted in figure 1(a), ω_p is lower than ω_0 and a saddle-like structure appears at the plasma edge. As ω_p increases (figure 1(c)), the plasma edge masks the additional oscillator, the saddle point becoming almost imperceptible (arrow), and the plasma edge slope changes. If ω_p is much lower than ω_0 (figure 1(b)), the additional oscillator is observable but it is not more pronounced because in 'strength' it is the weakest of all those considered (table 1). The values obtained for ω_p from table 1 are in accordance with the values obtained from transport measurements given in [8, 9, 11].

The $\omega_0(T)$-dependence depicted in figure 4 determines the energy difference between the one-electron and the two-electron states [9]. In figure 4, crosses correspond to the fitted spectra in figure 2(a), open circles to figure 2(b) and open

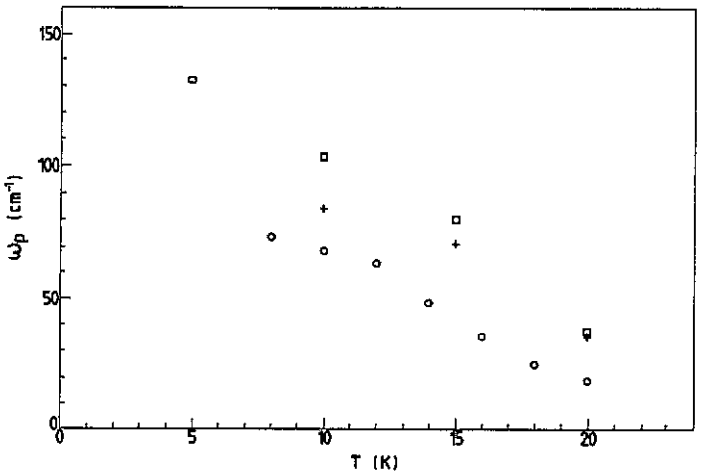

Figure 3. Temperature dependence of plasma frequencies: +, $N_{In} = 1.2$ at.%, $\Phi_1 = \Phi$; O, $N_{In} = 1.2$ at.%, $\Phi_2 = 0.75\Phi$; □, $N_{In} = 0.5$ at.%, $\Phi_3 = \Phi$.

squares to figure 2(*c*). An $\omega_0(T) = aT + b$ least-squares linear interpolation yields $a = -2.3 \times 10^{-4}$ eV K^{-1} and $b = 18.2$ meV, $a = \partial\omega_0/\partial T$ being the linear temperature shift coefficient of the energy difference between one- and two-electron states and $b = \omega_0(0)$ the extrapolated energy of the one-electron state at $T = 0$ K.

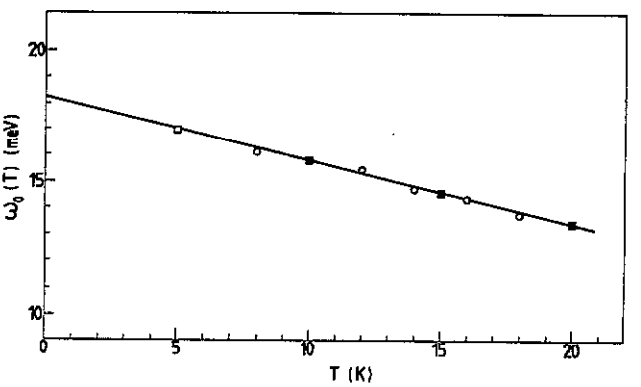

Figure 4. Temperature dependence of the additionally introduced oscillator characteristic frequency ω_0: +, $N_{In} = 1.2$ at.%, $\Phi_1 = \Phi$; O, $N_{In} = 1.2$ at.%, $\Phi_2 = 0.75\Phi$; □, $N_{In} = 0.5$ at.%, $\Phi_3 = \Phi$.

The $\omega_{loc}^2(T)/\omega_{loc}^2(0)$ curve is given in figure 5, with the same notation as in figure 3 for the experimental data. The oscillator strength ω_{loc}^2 is a function of the electron transition rate between the two-electron and one-electron localized states. It is easy to show that the normalized value $\omega_{loc}^2(T)/\omega_{loc}^2(0)$ is proportional to the temperature-dependent part on the transition matrix element M_{12}^2. The value of M_{12}^2 is in turn determined by the one-electron (excited) state lifetime τ_1 [12]. τ_1 depends on the probability W_e of electron emission from the one-electron state as $\tau_1 \sim 1 - W_e$. At low temperatures this emission is defined in terms of thermal activation via the barrier (E_g) between the one-electron (E_1) and two-electron (E_2)

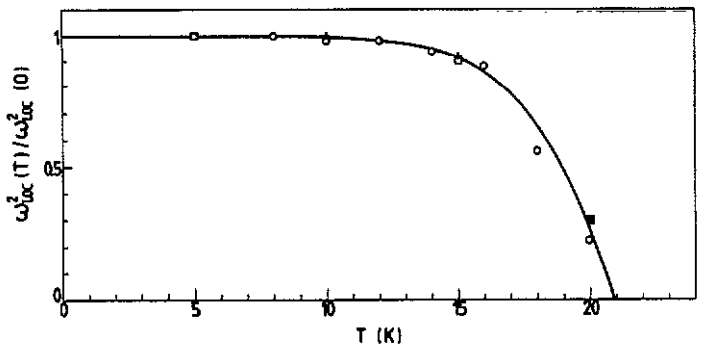

Figure 5. Temperature dependence of normalized 'strength' $\omega^2_{loc}(T)/\omega^2_{loc}(0)$ of the additionally introduced oscillator: +, $N_{In} = 1.2$ at.%, $\Phi_1 = \Phi$; ○, $N_{In} = 1.2$ at.%, $\Phi_2 = 0.75\Phi$; □, $N_{In} = 0.5$ at.%, $\Phi_3 = \Phi$.

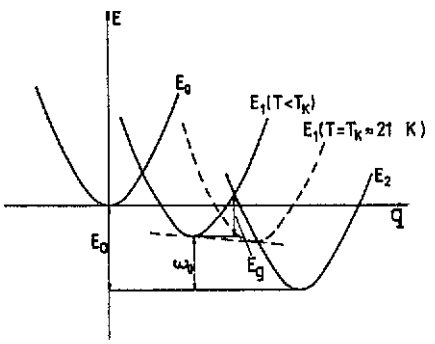

Figure 6. Configuration coordinate diagram for indium in $Pb_{0.75}Sn_{0.25}Te$.

localized states $W_e = \exp(-E_g/kT)$ (figure 6).

According to our scheme, the curve corresponding to the one-electron state moves as the temperature rises, and at $T = T_k$, the barrier between states E_1 and E_2 disappears (see the broken curve in figure 6). A good fit (full curve in figure 5) is obtained for

$$\omega^2_{loc}(T)/\omega^2_{loc}(0) = 1 - \exp(-E_g/kT) \tag{2}$$

where E_g is the two-electron-to-one-electron-state barrier width (see figure 6). A linear E_g–temperature dependence $E_g = A(T_k - T)$ results in a best-fit parameter of $E_g(\text{meV}) = 0.56(21 - T)$. Note that the value of $T_k = 21$ K coincides with the persistent photoconductivity temperature obtained from galvanomagnetic measurements [2, 8, 9, 11]. One can see that, at liquid-helium temperature, $E_g \gg kT$. Nevertheless, measurements of long-term photoconductivity relaxation show that the redistribution of the localized-state occupancies during this process plays an important role [13]. This means that at temperatures $T < 10$ K the main contribution to the transitions between E_1 and E_2 comes from tunnelling through the barrier E_g.

The universality of the $\omega^2_{loc}(T)/\omega^2_{loc}(0)$ curve indicates that the temperature-dependent part of the transition matrix element does not depend on the experimental conditions (light flux), nor does the interaction of the impurity centres affect the temperature-dependent part of intercentre transitions.

The impurity centre configuration state diagram is shown in figure 6. In accordance with the $\omega_0(T)$-dependence, the energy of the minimum that corresponds to the one-electron state is near the bottom of the conduction band (state E_1 in figure 6). The E_1-state occupancy is strongly temperature dependent ($\omega^2_{loc}(T)$), indicating a change in the barrier width between E_1 and E_2. At $T_k = 21$ K this barrier vanishes (broken curve in figure 6) and the related ω^2_{loc} drops to zero. The coincidence of this temperature with the temperature of the onset of the persistent photoconductivity effect supports our assumption that persistent photoconductivity depends on non-equilibrium charge-carrier relaxation via the one-electron metastable localized state.

4. Conclusion

The measurements of FIR reflectivity spectra discussed were performed on In-doped $Pb_{0.75}Sn_{0.25}Te$ single crystals in the temperature range 5–20 K for a variety of doping concentrations. We have shown that persistent conductivity depends on photo-excited electron relaxation via the metastable one-electron state. At $T < 21$ K, this state lies below the bottom of the conduction band and above the stable two-electron state. The potential barrier ($E_g(0) = E_{g0} = 11.76$ meV at $T = 0$ K) between these two states and its temperature dependence have been determined. The existence of the barrier is a pre-condition for the appearance of the persistent photoconductivity effect. We have also determined the position of the metastable one-electron in respect to the two-electron state (ω_0 at $T = 0$ K) and its temperature dependence.

Acknowledgments

The authors thank W König for the measurement of the FIR spectra, and A V Nikorich for samples.

References

[1] Ravich Yu I, Efimova B A and Smirnov I A 1970 *Semiconducting Lead Chalcogenides* ed L S Stil'bans (New York: Plenum) p 60
[2] Akimov B A, Ryabova L I, Yatsenko O B and Chudinov S M 1979 *Fiz. Tekh. Poluprov.* **13** 752 (Engl. Transl. 1979 *Sov. Phys.–Semicond.* **13** 441)
[3] Lent C S, Bowen M A, Allgaier R S, Dow J D, Sankey O F and Ho E S 1987 *Solid State Commun.* **61** 83
[4] Vul M, Voronova I D, Kalyuzhnaya G M, Mamedov T S and Ragimova T Sh 1979 *Zh. Eksp. Teor. Fiz. Pis. Red.* **29** 21 (Engl. Transl. 1979 *JETP Lett.* **29** 18)
[5] Adler P and Yoffa E J 1976 *Phys. Rev. Lett.* **36** 1197
[6] Akimov B A, Brandt N B, Klimonskiy S O, Ryabova L I and Khokhlov D R 1982 *Phys. Lett.* A **88** 483
[7] McKnight S W and El-Rayess M K 1984 *Solid State Commun.* **49** 1001
[8] Romčević N, Popović Z V, Khokhlov D R, Nikorich A V and König W 1991 *Infrared Phys.* **31** 225
[9] Romčević N, Popović Z V, Khokhlov D R, Nikorich A V and König W 1991 *Phys. Rev.* B **43** 6712
[10] Akimov B A, Brandt N B, Nikorich A V, Ryabova L I and Sokovishin V V 1984 *Zh. Eksp. Teor. Fiz. Pis. Red.* **39** 222 (Engl. Transl. 1984 *JETP Lett.* **29** 198)
[11] Akimov B A, Albul A V, Nikorich A V, Ryabova L I and Khokhlov D R 1984 *Fiz. Tekh. Poluprov.* **18** 1778 (Engl. Transl. 1984 *Sov. Phys.–Semicond.* **18** 1112)

[12] Ravich Yu I, Efimora B A and Smirnov I A 1970 *Semiconducting Lead Chalcogenides* ed L S Stil'bans (New York: Plenum) p 88

[13] Ivanchik I I, Khokhlov D R, Nikorich A V, Popović Z V and Romčević N 1990 *Proc. 8th Int. Conf. on Ternary and Multinary Compounds (Kishinev, 1990)* p 318